SEISMIC MICROZONING INVESTIGATIONS IN THE METROPOLITAN AREA OF SAN SALVADOR, EL SALVADOR, FOLLOWING THE DESTRUCTIVE EARTHQUAKE OF OCTOBER 10, 1986

Ezio Faccioli[1], *Corrado Battistella*[2], *Pietro Alemani*[2] *and Aldevis Tibaldi*[3]

ABSTRACT

An overview is given of the studies carried out for seismic microzoning purposes in the San Salvador city area after the most recent destructive earthquake of October 10, 1986. These include the assessment of a "reference earthquake" from historical and present seismicity, the elaboration of local subsoil models from existing geological and geotechnical data, the determination of dynamic properties of the local volcanic soils by in situ and laboratory tests, and the construction of seismic microzoning maps based on seismic response analyses and the strong-motion records written during the 1986 earthquake.

1. BACKGROUND AND SCOPE OF THE WORK

In few cities has the seismic history of the last centuries been as dramatic as in San Salvador, Central America. During the past 276 years, local shallow earthquakes have severely damaged this capital 11 times (not including the 1986 event) at intervals ranging from 2 to 66 years and averaging about 23 years (Harlow et al., 1988). The 1986 earthquake caused about 1500 victims, 100,000–150,000 homeless, and property damage initially estimated close to 1.5 billion US dollars

(1) *Department of Structural Engineering, Politecnico di Milano, Italy.*

(2) *Studio Geotecnico Italiano, Via Ripamonti 89 – 20141 Milano, Italy.*

(3) *Italtekna, Via Maresciallo Pilsudski, 124 – 00197 Roma, Italy.*

but probably reaching 2.0 billion (Olson, 1987). Following this event, which hit a small country already weakened by civil war and a deteriorating economy, a program of technical and social assistance, offered by the Italian government to help the recovery and reconstruction process, was accepted by the government of El Salvador. This program includes the construction of a new residential district for 20,000 people in the outskirts of San Salvador, the erection of a new children's hospital, and a host of technical, medical and social assistance measures aimed at the rehabilitation of some of the most depressed slum areas of the capital.

Given the severity of the natural hazards and the overpopulation problems in some of the most unfavorable areas, it was agreed by Salvadorian and Italian authorities that extensive geological, geotechnical and seismic investigations should be included in the previous program. The seismic investigations were carried out with the main objective of producing a reliable microzoning map and, as an intermediate product, appropriate geological and geotechnical maps of the study areas. The microzoning map was intended to identify stable and potentially unstable areas under strong earthquake shaking, and to quantify by appropriate parameters the level of expected seismic actions in stable areas, in such a way as to provide a suitable support to local seismic regulations and design practice. The geological work, including an assessment of volcanic hazard, was carried out by a separate team of specialists and produced geological, neotectonic and geomorphological maps, as well as cronostratigraphic criteria for near-surface soil formations, which could be used as an input to the seismic studies. For administrative and budgetary reasons, the microzoning investigations did not cover the whole metropolitan area of San Salvador (AMSS) but only a portion of it, officially named DS A3, corresponding to well over a half of the total area. The DS A3 includes most of the city center and a substantial part of the most damaged area in 1986 (see Figs.12 and 13).

The microzoning study, paralleled by geotechnical investigations aimed at standard characterization of local soils for foundation design and stability analyses, was carried out between January and July 1988 (a strict time limitation was imposed) with a nominal budget of about 300,000 US dollars. This includes all in situ and laboratory testing carried out for seismic characterization purposes.

2. SEISMOTECTONIC ENVIRONMENT, HISTORICAL AND RECENT SEISMICITY AFFECTING SAN SALVADOR

While the dominant tectonic feature, and the immediate or remote cause of earthquake and volcanic activity in the Middle America region is the subduction of Cocos Plate under the Caribbean Plate, see Figs.1-4, the severest hazard for El Salvador is historically represented by local shallow earthquakes of moderate size. These originate along a structural depression, called median trough ("fosa mediana"), which coincides with much of the active volcanic chain extending from Guatemala to Costa Rica over a length of about 1,100 km, see Fig.5. In addition to San Salvador and other population centers nearby, these shallow earthquakes have repeatedly destroyed or severely damaged the capitals of Guatemala (9 times) and Nicaragua, where the most recent earthquake (M_L 6.2, December 23, 1972) killed an estimated 20,000 people. Whereas many of these earthquakes occur near active volcanoes and some accompany volcanic eruptions, the significant ones have a tectonic origin, since strictly volcanic events are likely to have magnitudes $\leq$ 5.

Because of the high population density in and near San Salvador since at least 1700, recent studies have succeeded in reconstructing a complete earthquake history for this region. This includes 15 local events with estimated magnitudes $5.4 < M_s < 6.5$ between 1730 and 1899, and 6 local events with instrumentally determined magnitudes $5.4 < M_s < 6.4$ between 1917 and 1986 (Harlow et al., 1988). For these earthquakes, MM-VII intensity contours (encompassing areas of significant damage) were determined, as illustrated in Fig.6 a, b, c. From the size of the MM VII area for the events with instrumental magnitude, a correlation was found and used to estimate the magnitude of local earthquakes prior to 1910.

These data show that 6.5 is the historical upper limit of magnitude for local earthquakes in the San Salvador area, similar to other areas of the volcanic chain. Their temporal sequence provides an almost deterministic basis for estimating the return period of a damaging earthquake, which is of the order of 30-50 years for events with $6.0 < M_s < 6.5$. An event with these characteristics, and likely to occur anywhere between the San Salvador Volcano and Lake Ilopango (Fig.6), has been taken as the main reference earthquake for the

microzoning study. According to available correlations (Joyner and Boore, 1982), this earthquake would be capable of generating near-field peak accelerations of the order of 0.5 g. This essentially deterministic estimate can be compared with the results of a probabilistic hazard evaluation, which puts at 0.5 g and 0.6 g the peak accelerations corresponding to exposure times of 50 and 250 years, respectively, in San Salvador (Algermissen et al., 1988).

Some of the isoseismals in Fig.6 (e.g. 1839, 1854a) are elongated in a NW–SE direction, parallel to the dominant fault system in the volcanic chain region, while others (e.g. 1854b, 1919) have a transverse, or NE–SW elongation, which is parallel to the other main fault system. Other isoseismals still bear no evident relation to existing tectonic features. Thus, the seismic history does not suggest systematic relations of the earthquakes occurring in the median trough with a predominant fault system; rather, the two most recent events of 1965 and 1986 in the AMSS suggest that different causative faults, both in direction and extension, are activated each time. As to subduction zone events, White et al. (1987) report that they have damaged San Salvador only 4 times since 1700, the most recent one in 1982 (M_w 7.3). Since the minimum distance of the city from the subduction zone is 80 km (Fig.3), damaging effects are produced only by earthquakes with $M \gtrsim 7.0$.

Taking into account the existence of a significant gap along the coast of El Salvador (Fig.4), and the largest magnitudes along the Middle America arc, an earthquake with $M_s \simeq 8.0$ at a minimum distance of 80 km was selected as representative of subduction zone events. From available data and correlations (Idriss, 1978) for subduction zone earthquakes, it can be estimated that the previous event would produce a peak acceleration of about 0.30 g on competent soil in the San Salvador area, with a significant duration of the order of 30 s.

A third tectonic feature potentially relevant for San Salvador is the Motagua strike–slip fault, in Guatemala (Fig.1), which originated the M_s 7.5 destructive earthquake of February 4, 1976. This event, which was felt with I_{MM} V–VI and recorded with 0.05–0.07 g peak accelerations in the AMSS, is presumably representative of the largest earthquakes on the Motagua fault. Since the latter lies at a minimum distance ~150 km from San Salvador, its significance in terms of

seismic hazard for the city is not comparable either to the volcanic chain or to the subduction zone earthquakes.

3. THE 1986 EARTHQUAKE

The 1986 earthquake has provided invaluable data and observational evidence for the assessment of local seismic hazard in San Salvador. A comprehensive review of this earthquake is presented in "Earthquake Spectra", August 1987 issue, including seismological aspects and analysis of building damage. This was major and widespread for buildings in the three-to-seven story range, and the reported earthquake magnitude (M_s 5.4) does not appear to be consistent with the overall severity of damage and the strong-motion recordings (Anderson, 1987). The latter are the most important ever obtained in the AMSS and have been made readily available in digital form (Shakal et al., 1986). Prior to 1986, the most significant strong-motion record available for the AMSS was written during the June 19, 1982, M_w 7.3 subduction zone earthquake, at a focal distance of about 95 km, with a peak acceleration of 0.19 g and a significant duration of the order of 30 s at the Observatorio Sismológico station (Campbell and Algermissen, 1987).

The location of the accelerograph and seismoscope stations in the AMSS is shown in Fig.7. Station MDE malfunctioned while the OBS record could not be digitized. Except for station IVU, equipped with an AR-240 instrument, all other operational instruments were SMA-1's. Of the three instruments operating at HCR (Hotel Camino Real), only the basement record is considered in this study. The reported magnitudes for the main shock are M_s = 5.4 (NEIS) and M_w = 5.6 (White et al., 1987). If we compare the recorded values of the peak horizontal acceleration a_{max} with those predicted by one of the best available correlations (Joyner and Boore, 1982) for a moment-magnitude M_w = 5.6, it can be seen that the latter substantially underestimate the observations (Fig.8).

Using the synthetic Wood-Anderson seismograms obtainable from both horizontal components of the recorded accelerograms at 6 stations, we have recalculated the local magnitude by the method by Kanamori and Jennings (1978) obtaining the value M_L = 6.2±0.2. This is regarded as

an important result, since M_L is the magnitude measure most suitable for engineering applications. The recalculated value is more consistent with the actual severity of damage and provides a better prediction of observed a_{max} values, as shown in Fig.8. Moreover, given than M_L and M_s do not differ substantially in the 6.0–6.5 range, the recalculated magnitude implies that the 1986 event is representative of the local reference earthquake described in the previous section.

An additional check of the instrumental severity of the earthquake can be obtained from the seismoscope records which provide the value of the response spectrum ordinate at a nominal period of 0.75s and 10% damping. Using the values recorded at stations 3, 17, 18 (the only ones in Fig.7 which did not go off-scale) and at station 1 (IUSA, outside the limits of Fig.7), and taking the average after multiplication by the respective distances, as defined in Fig.8, the representative data point shown in Fig.9 is obtained for the pseudo velocity spectral ordinate (PSV). This can be compared to other data points associated with significant shallow earthquakes of the region also recorded by seismoscopes, notably the destructive 1972 Managua event (M 6.2) occurring in a similar seismotectonic environment, and to the values predicted by an appropriate correlation based on California earthquakes (Joyner and Boore, 1982). The M 6.2 value for the San Salvador event makes it quite consistent with the average of the available observations.

The San Salvador main shock, with a focal depth of 8 km, had a left-lateral strike-slip mechanism with a preferred rupture plane oriented N32°E (Fig.7) and a probable rupture length of 8–9 km (Harlow et al., 1988). The rupture plane, supported by the distribution of aftershocks, does not coincide with any of the mapped surface faults, and no coseismic surface faulting has accompanied the main shock, as was also the case in the previous destructive earthquake of 1965.

Strong ground shaking lasted for only 3 to 5 s and the main phase of motion consists of few strong pulses of low frequency (between 1 and 2Hz), relatively coherent throughout the AMSS. This is illustrated by plotting the horizontal acceleration components of all stations in the SH direction (normal to the epicenter-station direction), as in Fig.10. SH velocity components, not shown, display even better coherence. Note the very high value a_{max} = 0.72 g at station CIG, which is the nearest to the assumed rupture plane, and the relative

consistency of the peak acceleration levels at all other stations. Approximately the same is true for peak SH velocity, with a 72 cm/s maximum at CIG and values typically ranging between 35 and 47 cm/s at the other stations.

Local effects caused by the near-surface layers of softer pyroclastic materials are perhaps best seen in the acceleration response spectra, several of which exhibit distinct resonance peaks apparently corresponding to a varying thickness of the layers underneath the recording station. An extreme example of the differences in the spectra is given in Fig.11, but this type of data will be considered more extensively in a later section, in the context of microzonation proper.

The problem of strong ground motion prediction in the AMSS, however, is not confined to the local amplification caused by the soft pyroclastic materials, because the area is within the near field of the seismic source, and details of the rupture process can strongly affect the surface motions. As an example, soil response analyses suggest that the high peak motion values recorded at CIG, the station nearest to the causative fault, cannot be explained by local amplification alone. Furthermore, important aspects of the waveforms, resulting from the particle orbits (hodograph plots) in the horizontal plane, can be interpreted in terms of radiation from the rupture front as it progresses along the fault plane.

4. LOCAL GEOLOGY

The flat area on which the AMSS is located is sharply delimited to the NW by the San Salvador (Boquerón) volcano, to the N by Cerros de Mariona, and to the S by the inactive volcanic dome of Cerro San Jacinto. Further to the E is Lake Ilopango, a collapsed caldera with historical volcanic activity. The notable complexity of the local geology results from the superposition of materials erupted by different volcanic centers, characterized by both effusive and explosive type of activity. The stratigraphic section in the AMSS therefore consists of alternating volcanic and volcaniclastic rock sequences. The 1:5,000 geological and volcanological survey, carried out in the early part of 1988, has produced several advancements with

respect to the existing 1:15,000 geologic map prepared in 1968-69 by the Bundesanstalt für Bodenforschung of Germany for the local Centro de Investigaciones Geotécnicas (CIG). Based on the volcanologic analysis, the new survey has rectified in several aspects the predominantly stratigraphic framework of the previous study and has better defined the neotectonic activity. Because of their relevance in the seismic context, we summarize the basic elements of the stratigraphic succession, and refer to the geologic map of Fig.12.

Holocene. "Tierra Blanca" (auct.): pyroclastic flows, ash falls and surge beds which constitute a unit extending over most of the AMSS plain. They were deposited in successive eruptions from Lake Ilopango, as shown by the presence of several buried soil levels. The youngest deposit, named "Tierra Blanca Joven" (TBJ), has been dated at about 260 A.D. (Hart and Steen-McIntyre, 1983). The mechanical properties within this unit will be shown to be essentially constant.

Pleistocene. Upper Tuffs: pyroclastic flows, pumice and ash falls, white to gray in color, underlying the Tierra Blanca. They are mainly exposed along the cuts of deeply incised streams within the AMSS. The mechanical properties are comparable or better than those of the TBJ.

Lava flows of San Salvador volcano: andesitic-basaltic flows, exposed in streams beneath the Upper Tuffs unit, from the most recent eruption of the volcano towards the city.

Lava flows of Cerro San Jacinto: andesitic-acid to dacitic flows and dacitic domes, which constitute the bulk of the (inactive) volcano to the SE of the city.

Lower Tuffs: pyroclastic flows and ash falls, yellowish to reddish in color, cemented, sometimes agglomerated. They are exposed in limited areas to the S, along the Cadena del Bálsamo.

Alkaline lava flows: exposed in the Southern part of the AMSS plain, where they underlie the Tierra Blanca and Upper Tuff.

Pliocene-Pleistocene. Volcanic agglomerates, consisting of lava blocks in a clay matrix. This is the oldest unit exposed in the area, at the bottom of the deepest valleys in the Cadena del Bálsamo.

In addition to the previous stratigraphic units, one must consider the numerous uncompacted, artificial fills especially present along creeks and roads.

As to the tectonic characters, the AMSS area is intersected by two main fault systems, oriented NNW-SSE and ENE-WSW, which are also the youngest and correspond to the dominant longitudinal and transverse regional systems (Fig.5). The new geological survey has introduced a classification of the faults, depending on whether or not their most recent movements are posterior to the deposition of TBJ. In the geologic map of Fig.12 a different symbol and the legend "post Tierra Blanca Joven" has been used for the fault traces within the DS A3 with clear field evidence of activity posterior to TBJ deposition. The seismic significance of the surface faults in the AMSS is highly uncertain. Although a relation has been noted between some historical earthquakes and the orientation of different local faults, no clear association seems to exist between the source mechanisms of the most recent shallow earthquakes and the faults mapped at the surface. For these reasons, it was decided not to attribute a specific role, e.g. as seismogenic line sources, to the surface faults in the context of seismic microzoning. It seemed instead preferable, given the large number and close proximity of such faults, to consider the probability of occurrence of a damaging earthquake as uniformly distributed within the AMSS.

About 600 borings, for the most part not exceeding 12 m depth, have been collected and analyzed for the DS A3 area and neighbouring zones. These data allowed us to define a stratigraphic-structural model for shallow depths, which consists of an Upper Pyroclastic Unit, including the Tierra Blanca and Upper Tuffs, overlying the different types of lava flows and the Lower Tuffs. From the boring data, an isopach map of the Upper Pyroclastic Unit has been constructed, shown in Fig.13. This map introduces many significant changes with respect to a previous map of the same kind (Schmidt - Thomé, 1975) and can be used also for guidance in geotechnical investigations.

The definition of a stratigraphic-structural model at greater depth has proved a much more difficult task, because of its complexity and the scarcity of sufficiently deep borings. It has been ascertained that the exposed lava-flows not necessarily correspond everywhere to an effective seismic "bedrock" since they may extend into the subsoil

as thin, tapering layers. Furthermore, the deep subsoil has a graben structure and appears to be constituted by an irregular succession of lava-flows and pyroclastic materials with widely differing proportions and marked contrast in mechanical properties. With the support of the boring logs of 26 water wells in the DS A3, with depths ranging mostly between 100 m and 210 m, we have synthesized the subsoil characteristics at depth through a statistical representation of the cumulative thickness of the lava flows within 100 m from the surface. As shown in the map of Fig.14, based on the deep borings and the surface geology, two significantly different types of subsoil zone are identified, with the following characteristics:

- Cumulative thickness of lava flows < 35 m within 100 m depth, and
- Cumulative thickness of lava flows > 65 m within 100 m depth.

The depth and percentage limits being affected by inevitable arbitrariness, the following remarks are in order. The reference depth of 100 m is mostly dictated by the available data; whereas a depth corresponding to one-quarter wave length for a seismic wave period of 1 s might represent a more rational choice for seismic microzoning applications (Fumal and Tinsley, 1985), 100 m is believed to be a large enough value to account for the subsoil influence on the surface seismic response. Secondly, the 35 m and 65 m thresholds are also dictated by the boring data, and if these had been more numerous and more evenly distributed the sharp boundary between the two zones in Fig.14 would probably be replaced by some transition bands. However, the practical significance of the thresholds must be seen in relation to the anticipated seismic response. A site in this area with no exposed lava flows and with a cumulative thickness of lava of less than 35 m in the first 100 m (often subdivided in several thin layers far apart) will tend to respond seismically as a soft site. On the other hand, a site with more than 65 m of lava in the first 100 m will tend to respond either as a rock site (thick exposed lava flow), or as a resonant site if several m of soft material are present above the lava.

The representation adopted has proved useful in identifying anomalous areas, such as that shown near the upper left corner of Fig.14, which occurs within the main body of the most recent eruption of the San Salvador volcano towards the city, and might have been caused by irregularities in the preexisting topography.

Since the map of Fig.14 is probably the most important geological input for the microzoning work, its meaning and limitations should be kept in mind when evaluating the final results.

5. DYNAMIC SOIL PROPERTIES

The mechanical properties of the TBJ were evaluated in a first stage from the numerous SPT tests executed within the present project for the geotechnical characterization of local soils, illustrated in Fig.15. After an increase in the first few m, influenced by the frequent presence of superficial fills, the mean N_{SPT} value remains essentially constant (≈30) with a large scatter. Fewer data are available for the Upper Tuff soils, as illustrated in Fig.16. Here the scatter is even larger, but the mean value is only slightly greater than in the TBJ. This is not surprising, given the genetic affinity of these materials, and appears to justify the treatment of TBJ and Upper Tuffs as a single generalized unit from the engineering geology viewpoint (see Fig.13).

To fully characterize the seismic behavior of the local soils it was considered indispensable to determine the longitudinal and transverse propagation velocities, v_p and v_s, within the thickness range of the softer materials in the investigated area. Down-hole geophysical measurements to a maximum depth of 30 m were carried out for this purpose at 6 different locations, i.e. the four sites shown in Fig.12 and two additional ones in the Distrito Italia area (15 km from San Salvador, and with the same near-surface materials)(*). The measured v_s profiles are grouped in Fig.17, and these are the first in situ data so far obtained on the dynamic properties of the volcanic soils in the AMSS area. The three velocity profiles CIG, IGN, UCA were obtained at a few m distance from the accelerograph stations by the same name. Within about 20 m from the surface the measured S-wave

---

(*) The down-hole measurements were executed by a team headed by Dr. Y. Mok and supervised by Professor K. Stokoe, both of the University of Texas at Austin.

velocities for the TBJ and Upper Tuffs remain essentially constant or increase very mildly with depth, with mean values of 200–250 m/s. At greater depth, an increase occurs in correspondence with the older members of the Upper Tuff unit (as in HDN and IGN) or with scoriaceous/fractured parts of buried lava flows (as in UCA). Typical velocity values in the tuff materials below 20 m are of the order of 500 m/s. The strong velocity jump at about 11 m depth at CIG is due to a compact andesitic lava flow, which extends down to 28 m, and is underlain by softer tuffs.

Cyclic laboratory tests of the resonant column type were also performed to investigate the dependence of the dynamic shear modulus G and internal damping coefficient D on the cyclic shear strain amplitude γ; such relations constitute an essential input for analyses of seismic soil response. Undisturbed specimens for these tests were obtained from block samples taken in trial pits, or in exposed roadway cuts where the entire TBJ–Upper Tuff stratigraphic sequence is present (HDN area). The investigated materials were subdivided into two groups, depending mainly on their cementation, as follows:

Group A. Silty–clayey, uncemented or loosely cemented sands from TBJ layers at less than 5 m depth, with 5%–25% clay content.

Group B. Sandy silts (less than 5% clay content), from different buried soil levels within the Upper Tuff formation.

The experimental results for Group A soils are shown in Figs.18 and 19, where G_{max} is the shear modulus at very small strain. Its values (not shown in Fig.18) are in good agreement with in situ values obtained with the v_s measurements. The dynamic behaviour of TBJ soils is essentially elastic up to a threshold strain of about $2 \cdot 10^{-3}$%, and the modulus reduction vs. strain amplitude is well fitted by the Ramberg–Osgood model with the parameters shown in Fig.18. The data for Group B soils are similar to those of Group A, except for a smaller threshold strain (10^{-3}%) and a tendency for smaller damping values at large strains. The Ramberg-Osgood parameters for Group B soils were found to be A = 1.7, Z = 2.21 (see Fig.18 for definition).

In the seismic soil response analyses, all TBJ layers were characterized by the previous Group A curves for modulus and damping and all Upper Tuff layers and buried soils by the corresponding Group B curves.

6. SEISMIC MICROZONATION: GENERAL CRITERIA

A primary distinction was introduced between zones with predominantly stable seismic soil response and zones subject to different forms of instability. Since the main instability factors in the AMSS derive from active geomorphic processes in the erodible near-surface soils, the unstable areas were directly identified on the basis of the geomorphological survey executed at the scale of 1:5,000, and will be briefly described in a later section. No problems related with liquefaction apparently exist in the AMSS proper, chiefly because the main ground water table lies at depths exceeding 50 m and only the deepest streams intersect the aquifer. Sporadic water tables perched above the clayey, buried soils layers are apparently too modest to cause appreciable excess pore pressure effects. No liquefaction phenomena have been reported for the 1986 or the previous strong earthquakes in the city; the closest area to the AMSS where liquefaction evidence has been found, following the 1976 Guatemala earthquake, is the western shore of Lake Ilopango (Martinez, 1977).
In the stable zones the soils are expected to withstand the earthquake-induced stresses and accelerations without substantial permanent deformation, and the severity of ground motions can be suitably quantified by a reference horizontal elastic response spectrum (ERS) of acceleration at 0.05 damping. For convenience, the reference ERS, denoted by Sa, is described as a function of the natural period T by the following envelope

$$Sa\ (T) = A \cdot R_e\ (T) \qquad \ldots\ (1)$$

where A = effective peak horizontal acceleration (in g), and:

$$R_e\ (T) = \begin{cases} 1 + (R_o - 1)\ (T/T_1) & 0 \le T < T_1 \\ R_o & T_1 \le T < T_2 \\ R_o\ (T/T_2)^{-1} & T_2 \le T \end{cases} \qquad \ldots\ (2)$$

where T_1, T_2 are characteristic periods limiting the region of constant ordinate R_o. The ERS is therefore specified by a scale factor A, and the 3 shape factors T_1, T_2, R_o. Each stable microzone

will be associated with a different set of values of these parameters, while the vertical ERS will be taken as 2/3 of the horizontal one. This assumption is in good agreement with the vertical/horizontal ratio of a_{max} values recorded in 1986, but quite conservative with respect to the average shape of the recorded vertical spectra.
Consistent with the criteria underlying the construction of the deep subsoil map of Fig.14, the different zones indicated therein were identified as seismic microzones, namely:

Zone 1, roughly characterized by at least 65 m total thickness of lava flows within the first 100 m depth. It is subdivided in Zone 1A, where the lava flows are exposed or within 5 m from the surface, and Zone 1B, where they are found at a minimum depth ranging between 5 m and 35 m. The typical site response model for Zone 1B consists of a soft surface layer underlain by bedrock, with resonance periods varying with the layer thickness.
Zone 2, roughly characterized by less than 35 m total thickness of lava flows within the first 100 m depth. The seismic response in this zone will be more similar to that of deep soil sites, with longer dominant periods of motion than in Zone 1.

For the seismic characterization of these zones we have relied heavily on the 1986 recordings, integrated with numerical soil response calculations and with verifications based on data from subduction zone earthquakes. The choice of the numerical propagation model was guided by stratigraphic cross-sections based on available borings, even though these were largely insufficient in several areas, notably in Zone 2. Within a depth of some tens of m, the cross-sections show that a 1-D, horizontally layered soil model is adequate because the lateral variations in stratigraphy are mostly very mild over large distances (Fig.13). Hence, a standard numerical model for vertical shear wave propagation (Schnabel et al., 1972) was used, when needed. A situation at variance with the previous assumption can be seen (Figs.13-14) in the SE part of the DS A3, where the probable configuration of a narrow valley filled with relatively deep sediments would call for a 2-D soil model. This was discarded because of the lack of subsoil data and the building typology in the area, almost exclusively consisting of very modest 1-story constructions. Also, no

effort was made to model more complicated propagation phenomena, e.g. surface waves arising in connection with subduction zone earthquakes, due to the total lack of data on the deeper geological structure of the AMSS basin.

7. SEISMIC CHARACTERIZATION OF STABLE ZONES

Zone 1A

Since no strong-motion recording was written in this zone in 1986, we reduced by deconvolution from soil surface to exposed lava bedrock the SH accelerograms recorded at HCR, HSH and UCA stations, i.e. at sites belonging to Zone 1B where the lava flows lie at relatively shallow depth (10 m to 30 m). An example of deconvolution for the site HCR is given in Fig.20, while the average spectral shape (i.e. Sa/a_{max}) obtained from the three sites appears in Fig.21. This is compared with the corresponding curve yielded by the correlations of Joyner and Boore (1982) for rock sites, using the M = 6.5 upper bound magnitude assumed for the reference local earthquake and a distance d = 0 from the surface projection of the causative fault. Based on both curves, the values

$$T_1 = 0.2 \text{ s} \qquad T_2 = 0.5 \text{ s} \qquad R_o = 2.5$$

for the spectral envelope $R_e(T)$ of (2) were assigned to Zone 1A.
Using the most conservative reduction factors for peak acceleration calculated by deconvolution, the value of A (eq.(1)) for Zone 1A should be about 85% of the corresponding value for Zone 1B, or

$$A = 0.45 \text{ g}$$

Zone 1B

The 1986 recordings (SH components) at HCR, HSH and UCA are believed to be well representative of strong ground shaking in this zone, and were used directly to establish the ERS shape parameters as illustrated in Fig.22, namely:

$$T_1 = 0.3 \text{ s} \qquad T_2 = 0.6 \text{ s} \qquad R_o = 3.0.$$

Note the value of R_o, required by the high peak spectral responses at HCR and UCA and probably generated by soil resonance at the fundamental frequency of the surface soils. The value $R_o = 3.0$ and the assumed spectral shape are in excellent agreement with those yielded by the Joyner-Boore correlations for soil sites, $M = 6.5$ and $d = 0$ (not shown). The simple estimate $T_r = 4\,H/\bar{v}_s$ for the soil resonant period (H = thickness of soft layer, $\bar{v}_s$ = mean S-wave velocity) matches well the observed peak spectral periods, giving $T_r = 0.15$ s for site HSH ($H = 11$ m, $\bar{v}_s = 190$ m/s), 0.44 s for site HCR ($H = 21$ m, $\bar{v}_s = 190$ m/s) and 0.47 s for site UCA ($H = 34$ m, $\bar{v}_s = 290$ m/s).
The average value of recorded peak accelerations at the 3 previous stations, after correcting for zero distance from the surface projections of the causative fault, is 0.44 g. However, since all records were written at ground or basement level of multistory buildings, an upward correction of 20% was considered appropriate for free-field conditions, giving:

$$A \simeq 0.55 \text{ g.}$$

It should be noted that the peak mean value predicted by the Joyner-Boore correlations, irrespective of soil type, is approximately 0.5 g.

Zone 2

The representative 1986 accelerograms for this zone are those at IGN and CIG; the attribution of the latter site to this zone is suggested by the geological context, since borings are limited to 30 m depth and a lava flow occurs between about 11 and 28 m. The observed horizontal spectral shapes, obtained from the components as recorded, are shown in Fig.23 together with the assumed spectral shape, which is characterized by the values:

$$T_1 = 0.2 \text{ s} \qquad T_2 = 0.8 \text{ s} \qquad R_o = 3.$$

It is instructive to compare the assumed shape with those obtained from the OBS station (in Zone 2) strong-motion records of the June 19, 1982 subduction zone event, previously mentioned (Fig.24). The apparent unconservatism of the assumed ERS disappears when the acceleration factor A is taken into account, since the estimated

a_{max} = 0.3 g for the reference subduction zone event is much lower than the representative A value assumed for Zone 2, given below.
The average recorded peak acceleration value from IGN and CIG, after correction for distance as in Zone 1B, gives:

A = 0.55 g.

Other numerical tests of local soil response (not shown) were executed to verify the adequacy of the reference ERS vis-a-vis the effects of large, distant earthquakes, e.g. using as an input scaled versions of the 1952 Pasadena accelerogram (Kern County, California earthquake). All the results confirmed that the assumed ERS provides a confortable amount of conservatism.
The reference ERS attributed to the three stable zones are compared in Fig.25; the large difference between the spectrum of Zone 1A and the two others reflects the absence of local amplification on exposed lava flows and is consistent with the distribution of building damage caused by the 1986 event, as discussed below. The previous zones are shown in the proposed microzoning map for the DS A3, Fig.26.

8. UNSTABLE ZONES

Unstable zones, active or potential, have been identified on the basis of the most evident instability factors mapped in the separate geomorphological survey of the study area, in large part confirmed by the extremely numerous instability phenomena triggered by the 1986 earthquake (mostly of limited extent). The predominant factors identified in the microzoning map (Fig.26) include: active and old landslides, accelerated erosion or lateral erosion of stream banks, rockfalls and rockslides. Landsliding from the 1986 event caused an estimated 200 deaths, with most of damaged dwellings located within 10 m of stream banks or steep slopes. The most vulnerable and potentially hazardous areas are the densely inhabited rims of deeply incised streams and the stream banks, where the TBJ soils undergo very active erosion and are in a state of incipient failure. Upper Tuff materials, on the other hand, are less vulnerable to instability, due to cementation. As a result of the present investigations, it has

been recommended that no new dwellings should be allowed in these zones and that the existing ones be evacuated, but the possibility that any action will follow is objectively limited. Restrictions to new edification, recommended also for the areas subject to other instability factors, could be lifted after performing adequate case-by-case investigations and stability analyses showing an appropriate factor of safety.

A comprehensive review of instability phenomena triggered by the 1986 earthquake is given by Rymer (1987).

9. COMPARISON WITH THE 1986 DAMAGE DISTRIBUTION

The building damage distribution caused by the 1986 earthquake provides an interesting test for the proposed microzoning map. The results of a simplified survey, carried out by local engineers within the technical assistance program, are portrayed in Fig.27 for the most heavily damaged portion of the AMSS. Apart from the poorer dwellings (viviendas), nearly all of the surveyed buildings were at least two stories in height. Superimposed on the damage distribution in Fig.27 is the corresponding part of the microzoning map, limited to the stable zones for ease of representation.

The heaviest damage area lies almost entirely in Zone 1B and, by comparison with the isopach map of Fig.13, one may note that the thickness of the softer surface deposits in such area is between about 15 m and 25 m. According to the previous simple estimates and the numerical analyses, these values correspond to soil resonance periods between about 0.2 and 0.5 s, which is also an interval of high spectral response in the reference ERS for Zone 1B. The fact that damage was most severe to buildings in the 3-to-7 story range (Anderson, cit.), many of which are located in Zone 1B, suggests that the vibration periods of highest soil response were in the range of the fundamental periods of many damaged buildings. Thus, there appears to be some general agreement between the prediction of the proposed microzoning map and the 1986 earthquake damage in Zone 1B. The lack of damage in the western part of the city can be explained by different factors, such as a decreased severity of ground motions due to greater distance from the causative fault, better quality of

construction (mostly residential one-story buildings), and reduced thickness of soft soil. Damage was absent or very light in Zone 1A (only partially shown in Fig.27), which is also in agreement with the lesser severity of the corresponding reference ERS.

Relatively few significant buildings existed in Zone 2 and the most severely affected happened to be close to the surface projection of the causative fault. Several undamaged multistory buildings in Zone 2 were relatively recent and designed with some earthquake resistant criteria.

Despite the overall agreement, one must be cautions in evaluating the correspondence between the proposed microzoning map and the 1986 damage, because:

- The damage concentration visible in Fig.27 corresponds to the central area of the city, where the majority of the buildings more than two stories high were located.
- Many of the collapsed or severely damaged buildings in the central area had received only cosmetic repair, if any, after the damaging earthquake of 1965 and may had been further weakened by the strong earthquake of 1982.
- Damage in Zone 2 (i.e. the deeper soil zone with the highest spectral response at long periods) might have been more severe, had the 5-to-10 story buildings been more numerous.

10. RECOMMENDATIONS ON SEISMIC DESIGN ACTIONS

The reasons justifying a reduction of the ERS ordinates for design purposes are particularly evident for the local shallow earthquakes in San Salvador, since the strong shaking duration does not exceed a few seconds and the number of significant loading cycles is quite reduced (1 to 3 cycles in 1986). As to the less frequent subduction zone earthquakes, it was noted that scaling the 1982 response spectrum at OBS (Fig.24) to a peak acceleration of 0.3 g results in a spectrum with ordinates 1.5 to 2.0 times smaller than those of the reference ERS for Zone 2. It can therefore be assumed that, even if the subduction earthquakes duration is much longer than that of the local ones, the difference in spectral ordinates still makes the latter more unfavourable.

To provide quantitative guidance in the selection of reduction factors we have analyzed the response of simple elastic and elastoplastic 1-DOF systems with 5% damping to a base excitation represented by the IGN-EW acceleration component (probably the most severe among those recorded in 1986). The yield limit in the elastoplastic system was taken equal to 1/4 of the force required for a fully elastic response. The results show that the peak displacement of the elastoplastic system is typically twice as large as the yield displacement and about 1/2 of the peak displacement of the elastic system. An example of the elastoplastic force-displacement response is illustrated in Fig.28 for a system with initial natural period of 0.8 s. There is only 1 1/2 cycle of significant inelastic deformation, after which the system undergoes asymmetric elastic oscillations with a final residual displacement of 4 cm. Similar results are obtained for other natural periods and different 1986 accelerograms, thus showing that 1-2 cycles of deformation are enough to damp out the motion of a structure subjected to this type of excitation. These simple analyses indicate that a ductility factor of about 2 would suffice for the structure to resist the earthquake, and this implies a ductility demand about one-half of that resulting from accelerograms such as El Centro 1940, adopted in other seismic regions to obtain the design spectra.

Taking into account the construction and quality control standards predominant in San Salvador, it seemed preferable to recommend reductions in the ERS ordinates which are moderate with respect to those allowed by the previous theoretical calculations, without introducing stringent requirements for high ductility.

We have therefore proposed to start from a "design elastic spectrum" (DES) which is obtained by dividing by 2.75 the ordinates of the reference ERS, by extending to T=0 the spectral plateau and by taking the ordinate reduction beyond T_2 proportional to $T^{-2/3}$ (rather than T^{-1} as in the ERS). This first reduction accounts for the over-strength and additional damping of real structures with respect to computational models, and is similar to that introduced in the 1988 version of the American Uniform Building Code. The resulting DES for Zones 1B and 2 are shown in Fig.29. The DES are further reduced for ductility, depending on the structural systems. For usual r.c. and steel structures with frames and shear walls, the recommended

ductility factor is 10/3, so that the maximum seismic coefficient is 0.12 for Zone 1A and 0.18 for Zones 1B and 2 (Fig.29). A smaller reduction obviously applies for structures of reduced ductility, such as reinforced or unconfined masonry, so as to obtain a maximum seismic coefficient of 0.27. For structures where both design and supervision criteria during construction ensure a high ductility level, a larger reduction can be allowed, so as to give a maximum seismic coefficient of 0.12 in Zones 1B and 2.

From 1966 to 1986, the basic lateral coefficient for framed structures prescribed by seismic regulations (not enforced by law) in San Salvador was 0.12. After the 1986 earthquake an emergency seismic design code, published by the local association of engineers and architects, recommends a coefficient of 0.10(steel) – 0.12(r.c.) for framed structures. In the light of the previous considerations and of the performance of existing buildings during the 1986 earthquake, we believe that the previous values imply excessive reductions with respect to the prevailing design and construction practice for ductility.

CONCLUSIONS

Seismic microzoning of a large urban area exposed to severe seismic and geologic hazard is a complex multidisciplinary undertaking. The main aim of this paper is to illustrate the broadband spectrum of the research activities involved (including seismology, geology, and geotechnical and structural earthquake engineering) and their close interconnection. Although time and budget limitations have precluded some desirable developments, we believe that we have provided a usable tool for earthquake hazard mitigation to urban planning authorities and professional engineers of San Salvador. Under normal circumstances some crucial mitigation measures, especially in the unstable zones, could be taken more as a matter of common sense than as the result of sophisticated studies. However, the social and economic reality of San Salvador poses almost unsurmountable difficulties in this respect. On the other hand, the present awareness of local engineers that a clearer identification of the hazards and better design tools are being provided makes one hope that a gradual

improvement in siting and in the earthquake resistant quality of constructions is developing. Although the microzoning study needs to be extended to the entire metropolitan area of San Salvador, and to be strengthened by better knowledge of the deeper geologic structure and seismically active tectonic lineaments of the region, we would be contented if in the meantime our work contributed to develop in all those responsible a more realistic appreciation of the effects of the next destructive earthquake.

Acknowledgments

The San Salvador seismic microzoning project was carried out by Studio Geotecnico Italiano (SGI), Milan, under a contract with Consorzio Salvador E. (Italtekna - Italconsult), Rome, financed by Italy's Ministry of Foreign Affairs, General Branch of Cooperation to Development. The field geologic and geomorphologic surveys were executed under a separate contract by Società Geotermica Italiana, Pisa, with the coordination of A. Frullani, who closely cooperated with us. The advice of R. Meli, of UNAM Institute of Engineering, Mexico City, for recommendations on seismic design spectra is gratefully acknowledged. We express our gratitude to the SGI staff, and in particular to F. Picco, geologist, and to C. Ramella and V. Manerba for the production of the manuscript.

REFERENCES

ALGERMISSEN S., HANSON S., THENHAUS P. (1988). Seismic Hazard Evaluation of San Salvador, El Salvador. U.S. Geological Survey Report, prepared for USAID.

ANDERSON R. (1987). The San Salvador Earthquake of October 10, 1986. Review of Building Damage. Earthquake Spectra, 3, 497-542.

BURBACH G., FROHLICH C., PENNINGTON W., MATUMOTO T. (1984). Seismicity and Tectonics of subducted Cocos Plate. Journ. Geophys. Res. 89 (B9), 7719-7735.

CAMPBELL K., ALGERMISSEN S. (1987). Processed Strong-motion Data for the El Salvador Earthquake of June 19, 1982. Open-file Report 87-xxxx, U.S. Geological Survey, Denver, Colorado.

CARR M. (1976). Underthrusting and Quaternary faulting in Northern Central America. Geologic. Soc. America Bull., 87, 825-829.

CARR M., STOIBER R. (1977). Geological Setting of some Destructive Earthquakes in Central America. Geologic. Soc. America Bull., 88, 151-156.

FUMAL T., TINSLEY J. (1985). Mapping Shear-Wave Velocities of Near-Surface Geologic Materials. Evaluating Earthquake Hazards in the Los Angeles Region. An Earth-Science Perspective (Ziony J. editor). U.S. Geological Survey Prof. Paper 1360, Washington, 127-149.

HARLOW D., WHITE R., RYMER M., ALVAREZ S., MARTINEZ C. (1988). The San Salvador Earthquake of 10 October 1986 and its Historical Context. Science.

HART W., STEEN-McINTYRE V. (1983). Tierra Blanca Tephra from the AD 260 Eruption of Ilopango Caldera. Archeology and Volcanism in Central America: The Zapotitan Valley of El Salvador (Sheets P. editor). University of Texas Press, Austin, Texas, 14-43.

IDRISS I. (1978). Characteristics of Earthquake Ground Motions. Proc. ASCE Specialty Conf. on Earthquake Eng. Soil Dynamics, Pasadena, Vol.III, 1151-1265.

JOYNER W., BOORE D. (1982). Prediction of Earthquake Response Spectra. Open-file Report 82-977, U.S. Geological Survey, Menlo Park, California.

KANAMORI H., JENNINGS P. (1978). Determination of Local Magnitude, M_L, from strong-motion accelerograms. Bull. Seism. Soc. Am., 68, 471-485.

MARTINEZ M. (1977). Repercusiones del terremoto de Guatemala en la Repùblica de El Salvador. Boletin ASIA, n.44, 22-35, San Salvador.

McCANN W., NISHENKO S., SYKES L., KRAUSE J. (1979). Seismic Gaps and Plate Tectonics: Seismic Potential for Major Boundaries. Pageoph, Vol.117, 1082-1147.

OLSON R. (1987). The San Salvador Earthquake of October 10, 1986. Overview an Context. Earthquake Spectra, 3, 415-418.

RYMER M. (1987). The San Salvador Earthquake of October 10, 1986. Geologic Aspects. Earthquake Spectra, 3, 435-463.

SCHMIDT-THOME' M. (1975). The Geology in the San Salvador Area (El Salvador, Central America), a Basis for City Development and Planning. Geologisches Jahrbuch, V.13, 207-228.

SCHNABEL B., LYSMER J., SEED H. (1972). SHAKE: a Computer Program for Earthquake Response Analysis of Horizontally Layered Sites. Rep. E.E.R.C. 72-12, Earthq. Eng. Research Center, Univ. California, Berkeley.

SHAKAL A., HUANG M., PARKE D., LINARES R. (1986). Processed Strong-Motion Data from the San Salvador Earthquake of October 10, 1986. Report OSMS 86-07, Office of Strong Motion Studies, California Dept. of Conservation, Sacramento, California.

WEBER H., WIESEMANN G., LORENZ H., SCHMIDT-THOME' M. (1978). Mapa Geològico de la Repùblica de El Salvador/America Central. Bundesanstalt Geowissenschaften und Rohstoffe, Hannover, Germany.

WHITE R., HARLOW D., ALVAREZ S. (1987). The San Salvador Earthquake of October 10, 1986. Seismological Aspects and Other Recent local Seismicity. Earthquake Spectra, 3, 419-434.

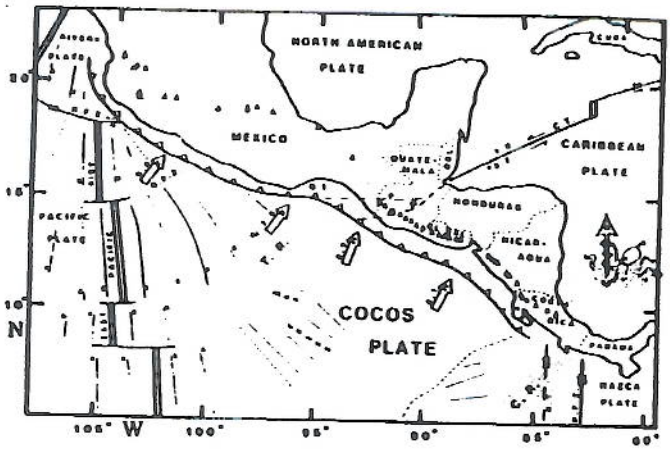

Fig.1

Tectonic framework of Middle America Region. Triangles indicate active volcanoes, arrows with a C indicate motion of Cocos Plate relative to the Caribbean Plate (7-8 mm/yr). Dashed lines crossing Guatemala are the Polochic and Motagua faults. After Burbach et al. (1984).

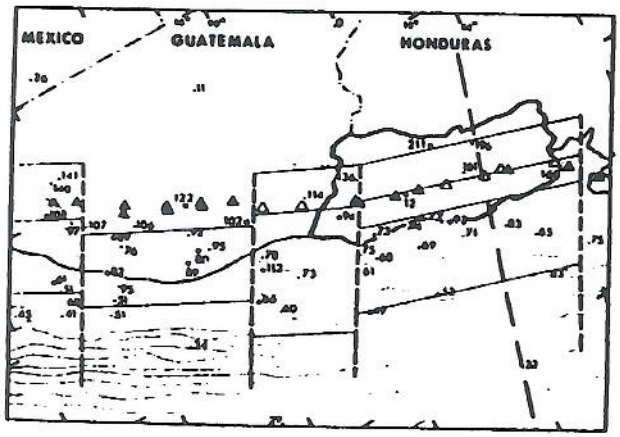

Fig.2

Seismicity 1965-1970 in El Salvador and Guatemala, with focal depths in km written next to earthquake epicenters (dots). Straight lines are isobaths of the subduction seismic zone, with 50 km contour intervals. Solid triangles are volcanoes with historic eruptions. Unlabeled country is El Salvador. Dashed line on the right locates cross-section of Fig.3. After Carr (1976).

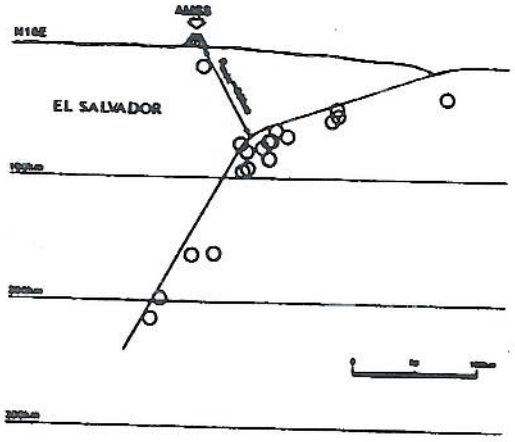

Fig.3

Vertical cross-section of earthquake foci in El Salvador, see Fig.2. The volcano (AMSS) gives the position of San Salvador. Line enveloping the foci is the profile of the subduction zone, from Burbach et al. (1984). Its minimum distance from AMSS is 80 km. After Carr (1976).

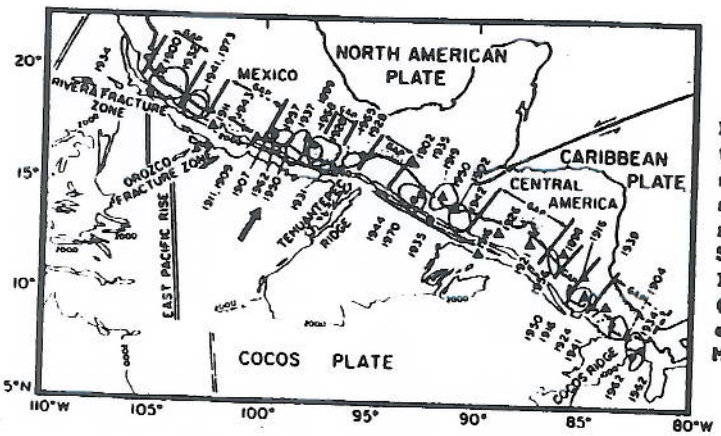

Fig.4

Rupture zones (ellipses) and epicenters (triangles and circles) of large shallow earthquakes, mainly from the subduction zone, along the Middle America Arc. Note wide seismic gap in El Salvador; earthquakes of 1921 (M_s 7.3), 1926 (M_s 7.1), both shown, and of 1982 (M_s 7.0), not shown, did not have enough energy to fill this gap. From McCann et al. (1979).

Fig.5

Structural setting of moderate shallow earthquakes in Guatemala, El Salvador and Nicaragua. Dashed lines show longitudinal (i.e. parallel to the volcanic chain) fault zones, and transverse ones. Circles mark locations of well described destructive earthquakes. After Carr and Stoiber (1977).

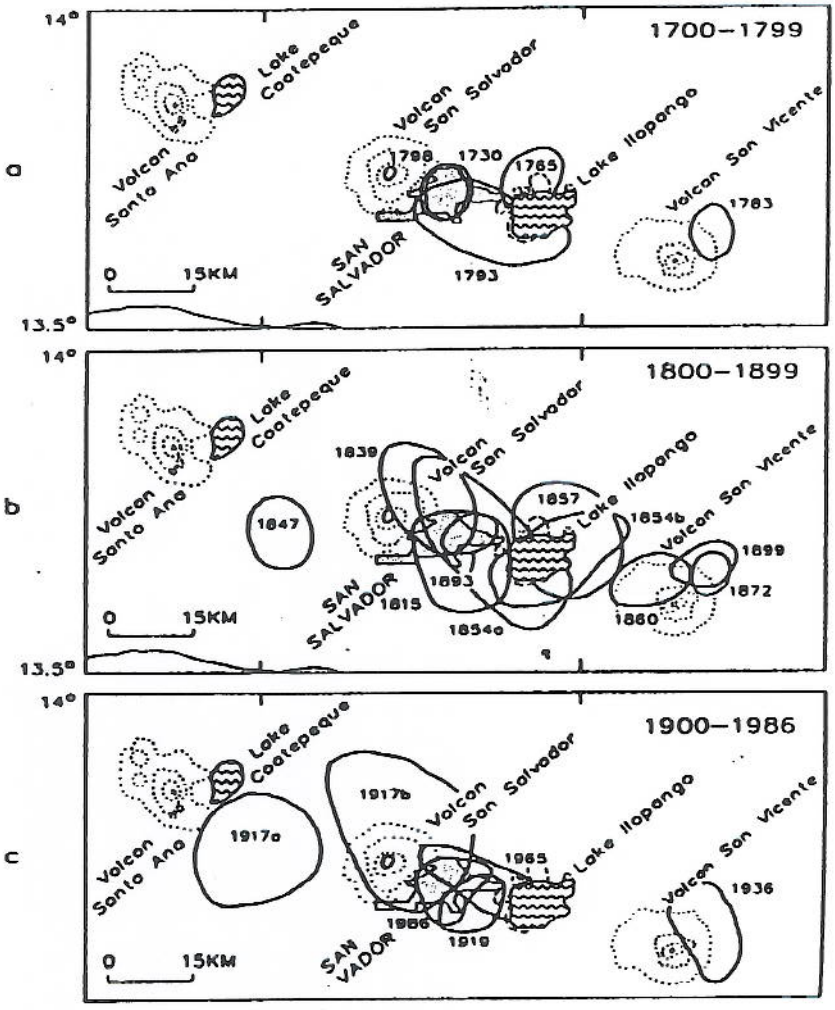

Fig.6

a,b,c: Maps with MM ≥ VII contours and dates for damaging shallow earthquakes within 50 km of San Salvador for the period 1700-1986. Shaded area is the AMSS. From Harlow et al. (1988).

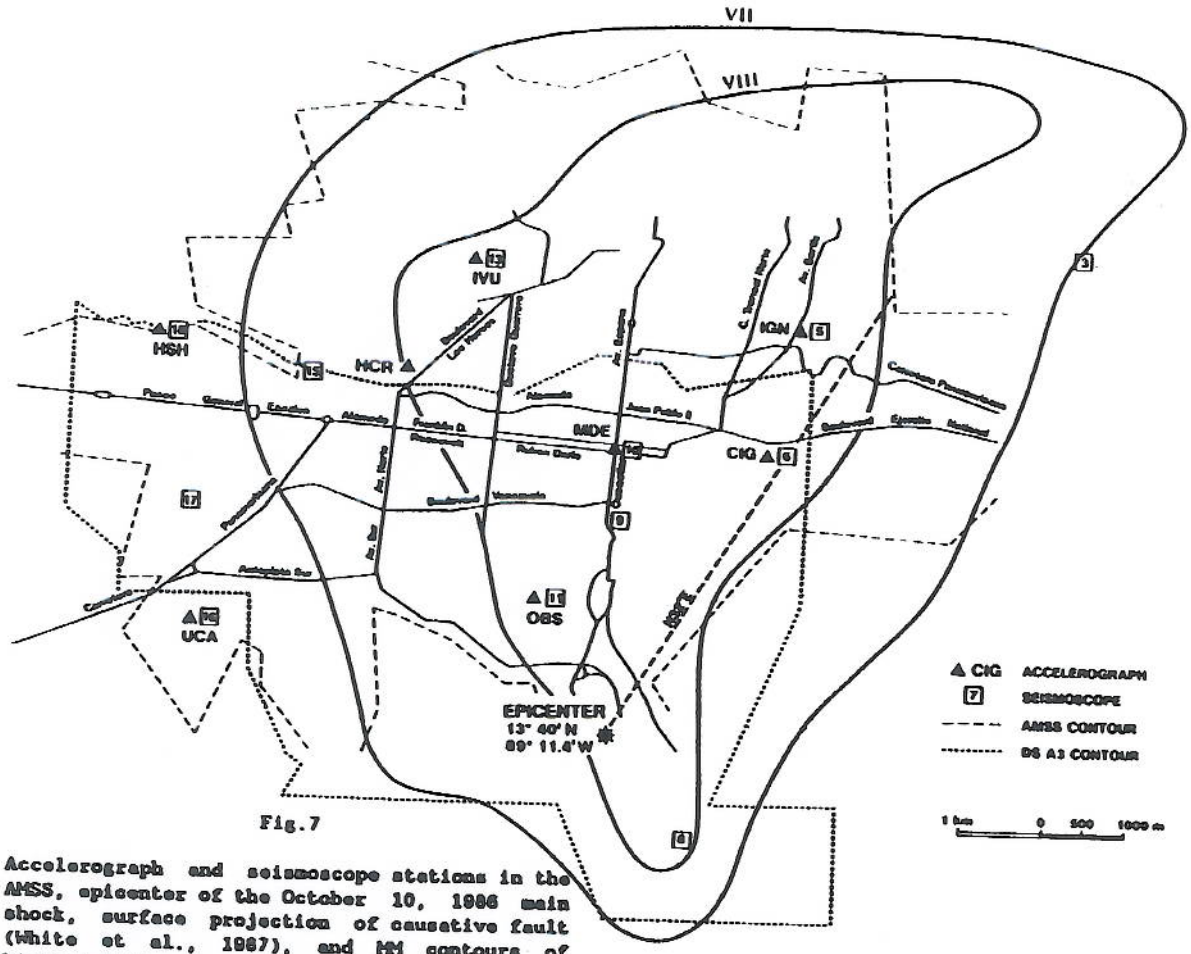

Fig.7

Accelerograph and seismoscope stations in the AMSS, epicenter of the October 10, 1986 main shock, surface projection of causative fault (White et al., 1987), and MM contours of highest degree isoseismals.

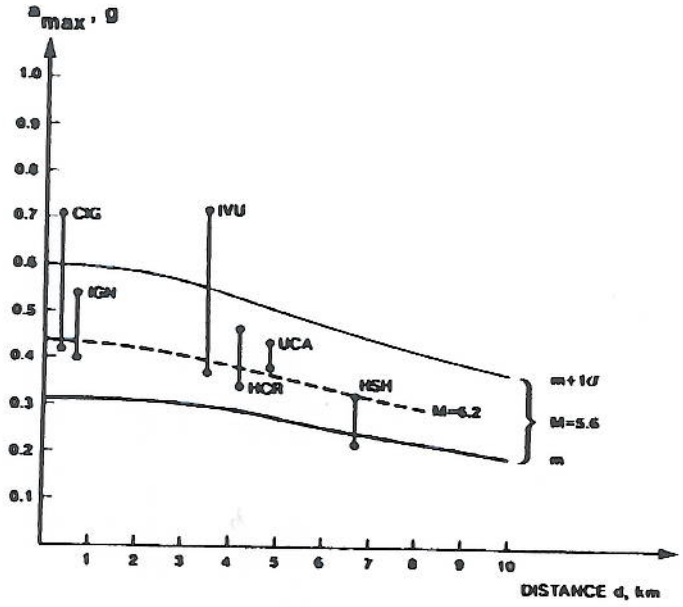

Fig.8

Horizontal a_{max} values recorded during the 1986 main shock in the AMSS as a function of shortest distance d from surface projection of causative fault (shown in Fig.7). Continuous and dashed curves are predictions given by Joyner and Boore (1982) correlation, for different magnitudes. m=mean value, σ=standard deviation.

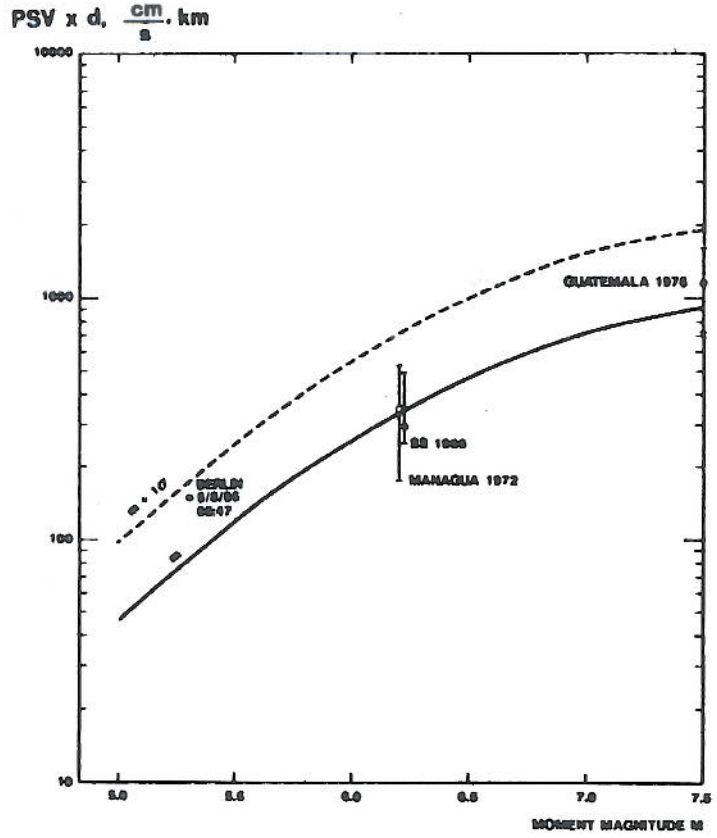

Fig.9

Magnitude dependence of the average pseudo-velocity (PSV) spectral ordinate at 0.75 s period and 0.10 damping. The data points for Central America earthquakes (recorded by seismoscopes) are compared to prediction curves (Joyner and Boore, 1982) based on California earthquakes.

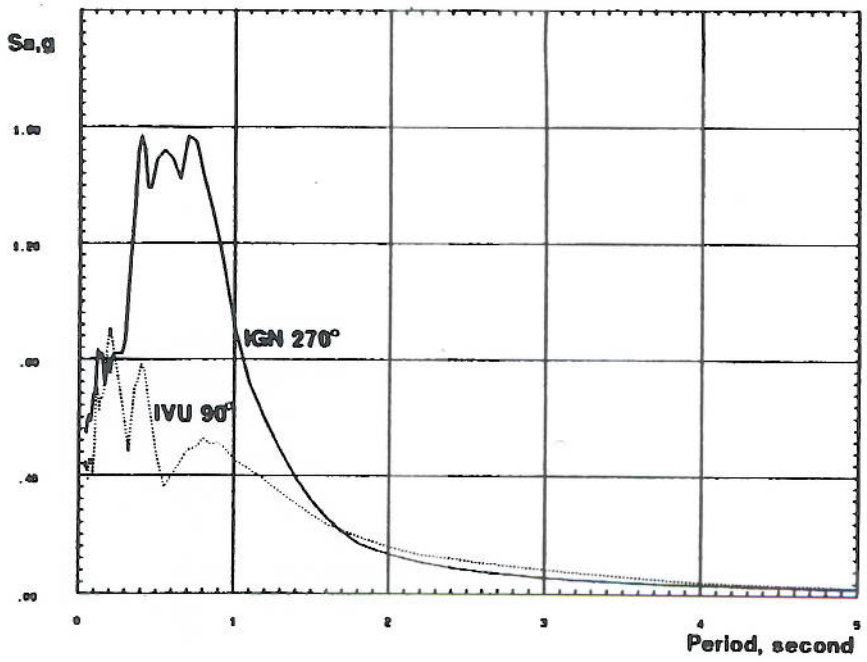

Fig.11

Examples of horizontal acceleration response spectra of 1986 event at stations IGN and IVU, for 0.05 damping.

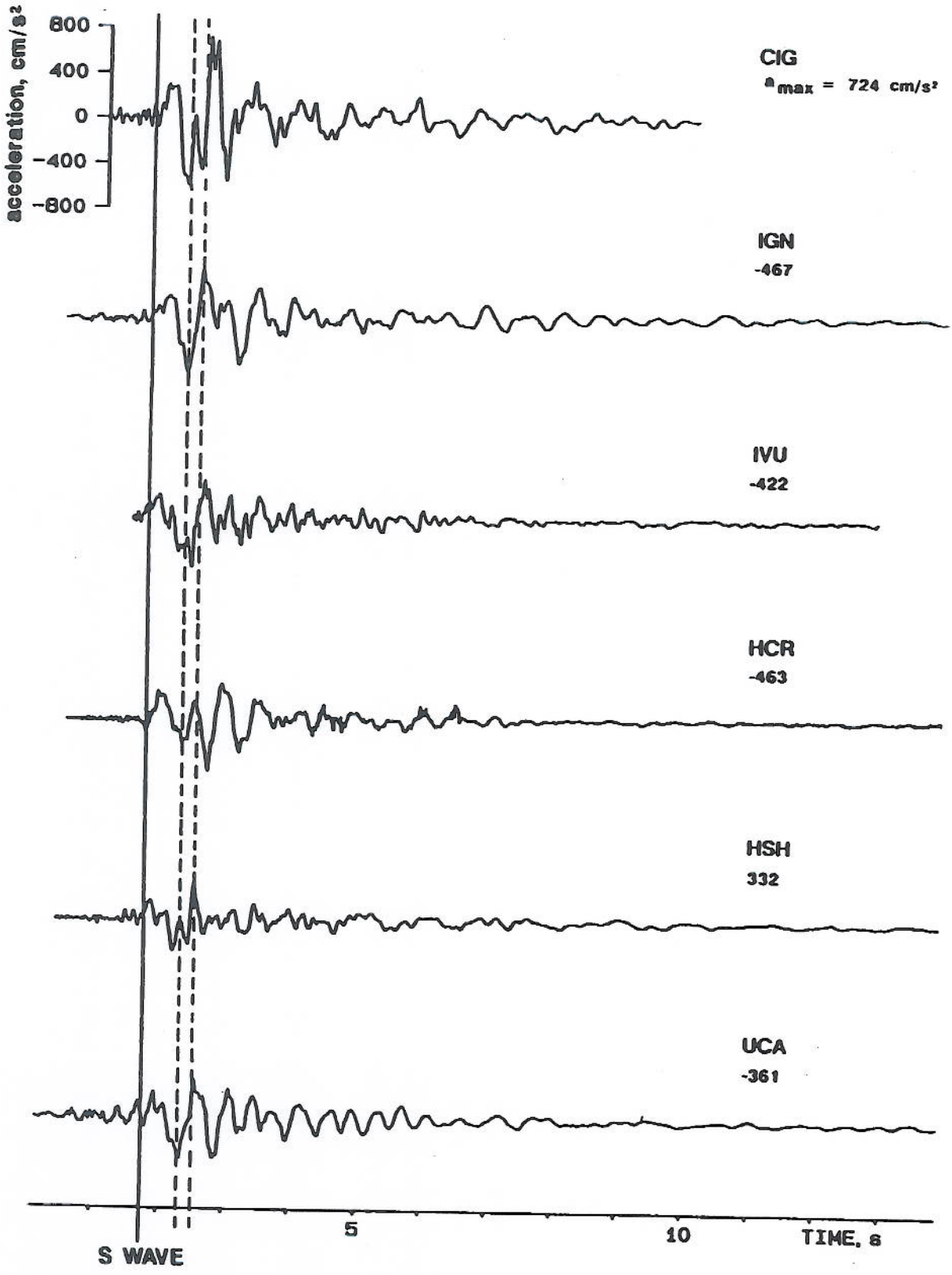

Fig.10

SH acceleration components in AMSS from the 1986 main shock. The seismograms are vertically aligned at interpreted onset of direct S wave from the source (continuous line); other coherent peaks are also shown (dashed lines).

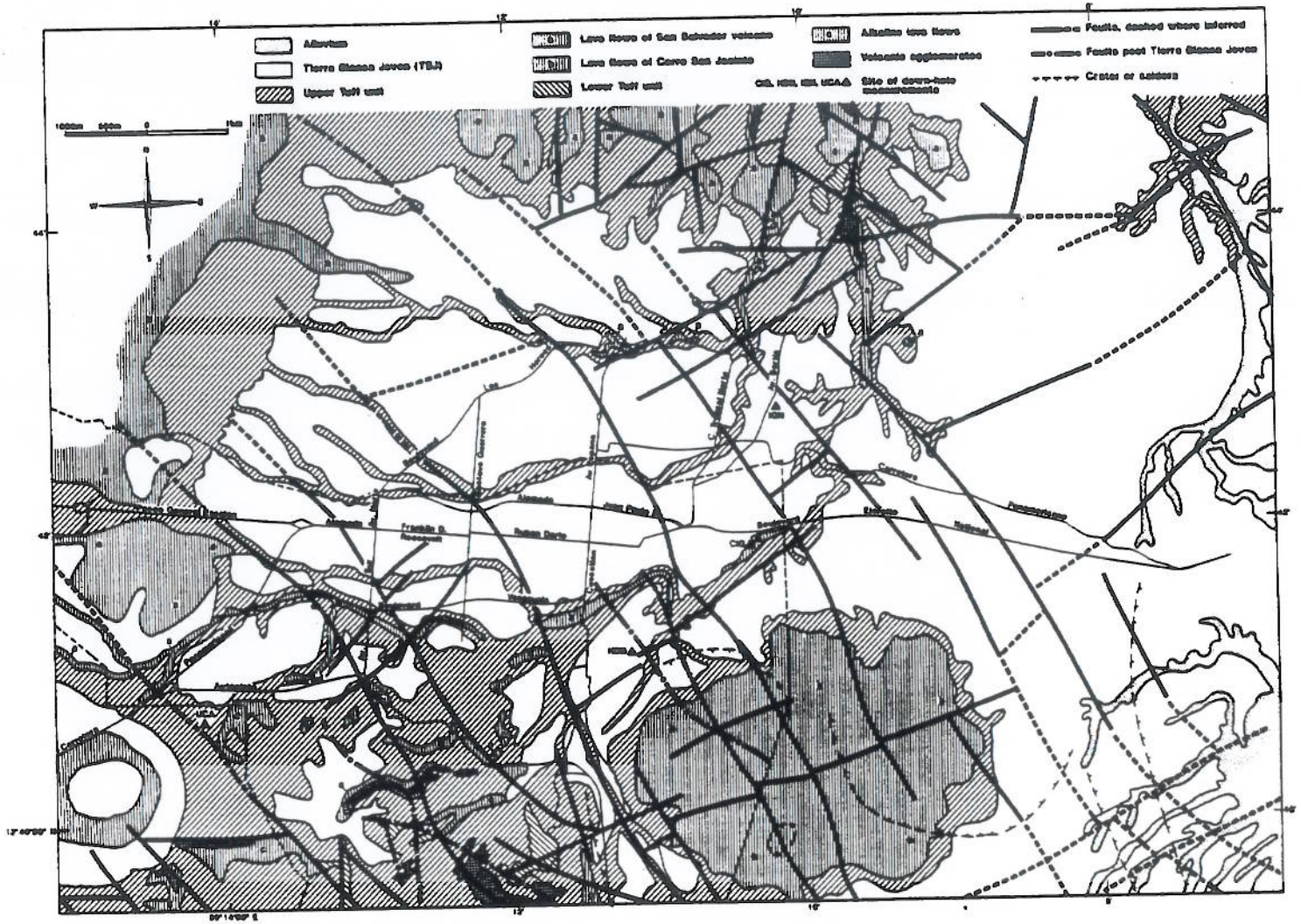

Fig.12. Geologic map of the San Salvador area (AMSS). Dashed contour at lower left side marks the DS A3 district where new geological survey and microzoning study were carried out. Portion of map outside DS A3 modified from Weber et al. (1978).

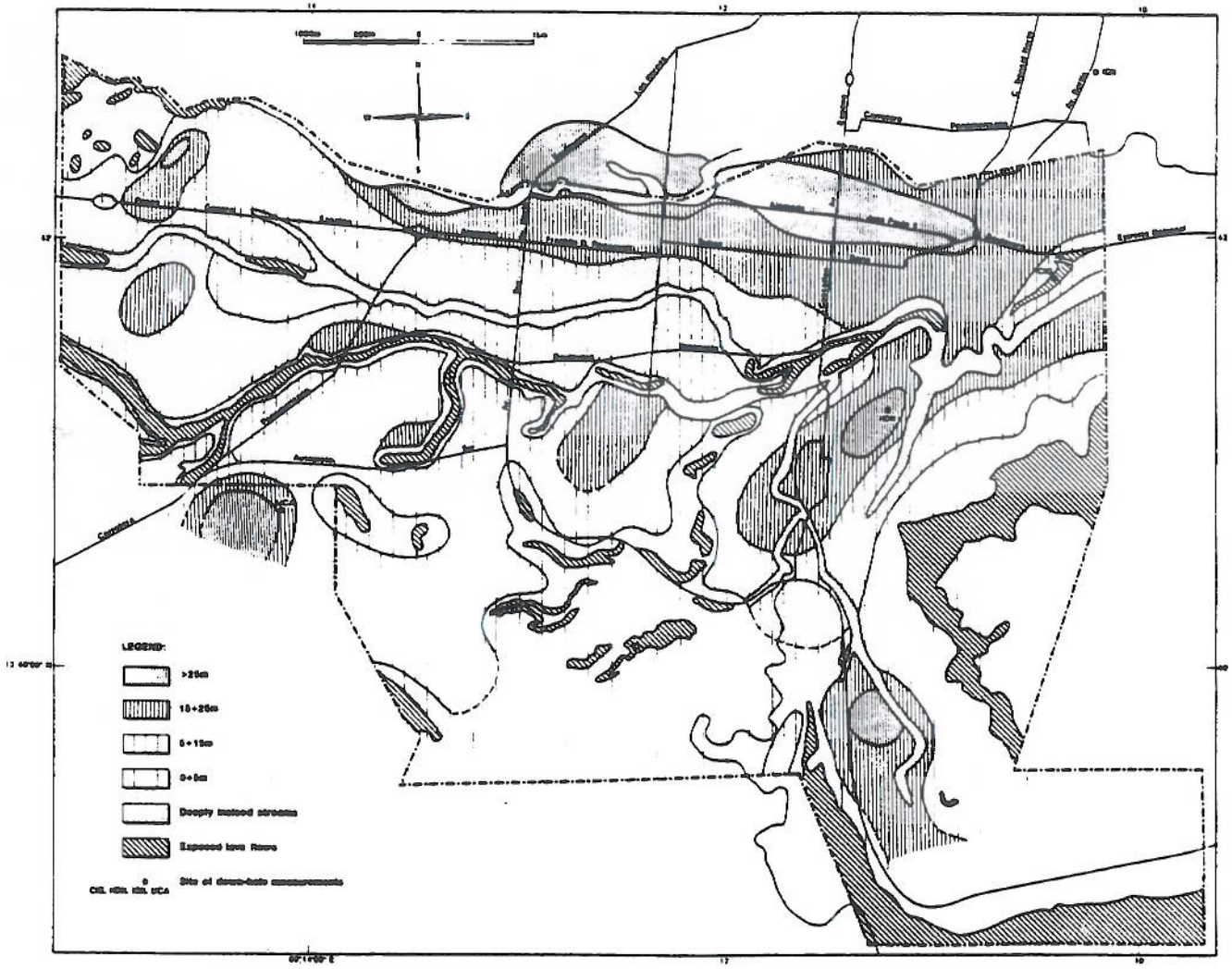

Fig.13. Isopach map of generalized Upper Pyroclastic unit, including Tierra Blanca and Upper Tuffs, within the DS A3 district of AMSS, contoured in Fig.12. Map is based on data from about 600 borings at 107 different sites. The contours are dashed where inferred.

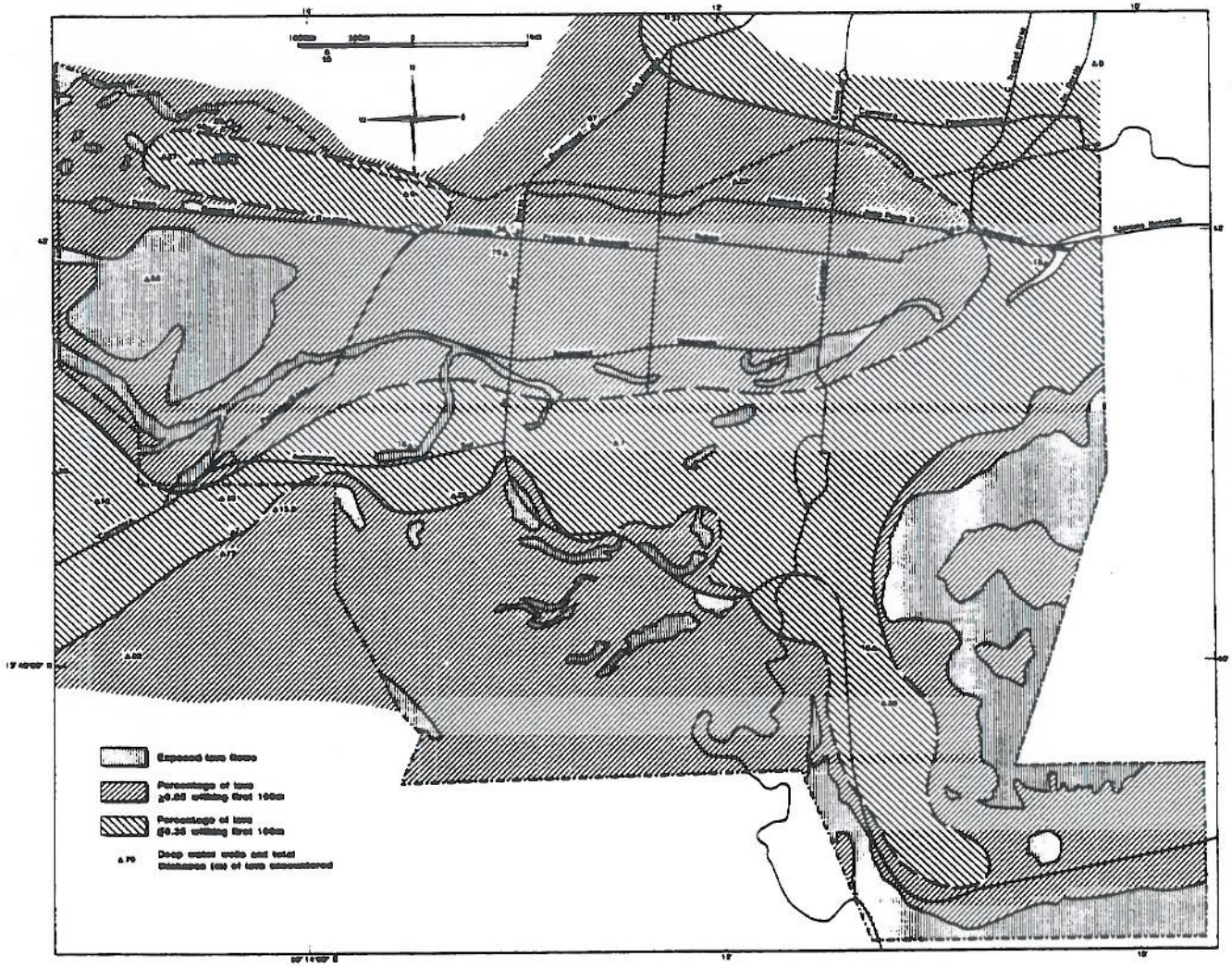

Fig.14. Distribution of the cumulative thickness of lava flows within 100 m depth from ground surface (in percentage) within the DS A3, based mostly on the boring logs of deep water wells. The zone contours are dashed where inferred.

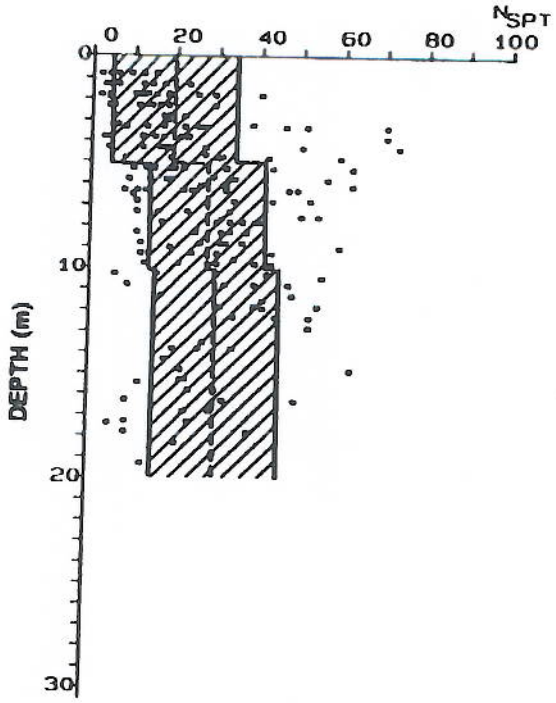

Fig.15

Data from SPT tests in 28 borings in Tierra Blanca Joven, with mean values and ±1σ bands.

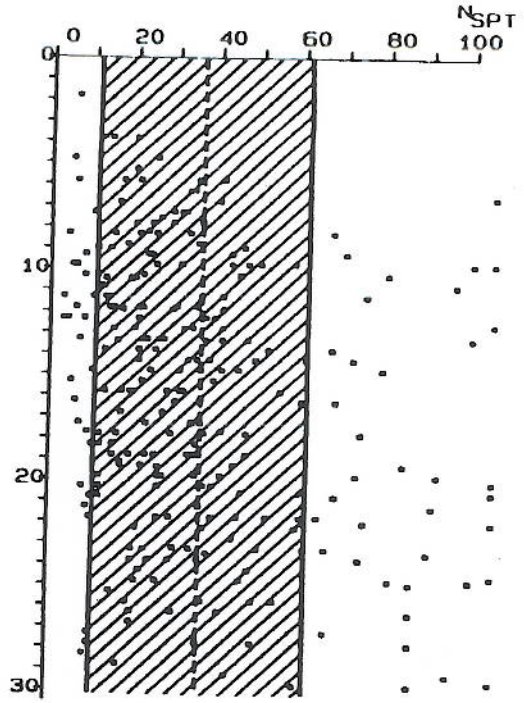

Fig.16

Data from SPT tests in Upper Tuffs, with mean value and ±1σ bands.

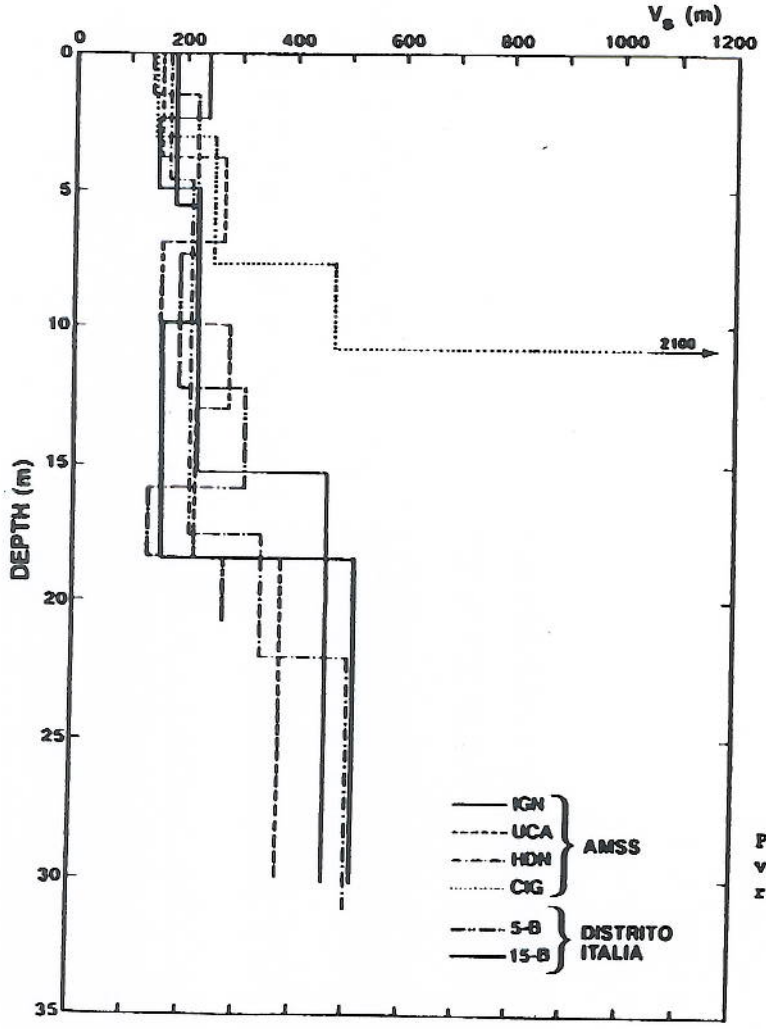

Fig.17

Profiles of shear wave propagation velocity v_s from down-hole measurements at 6 sites.

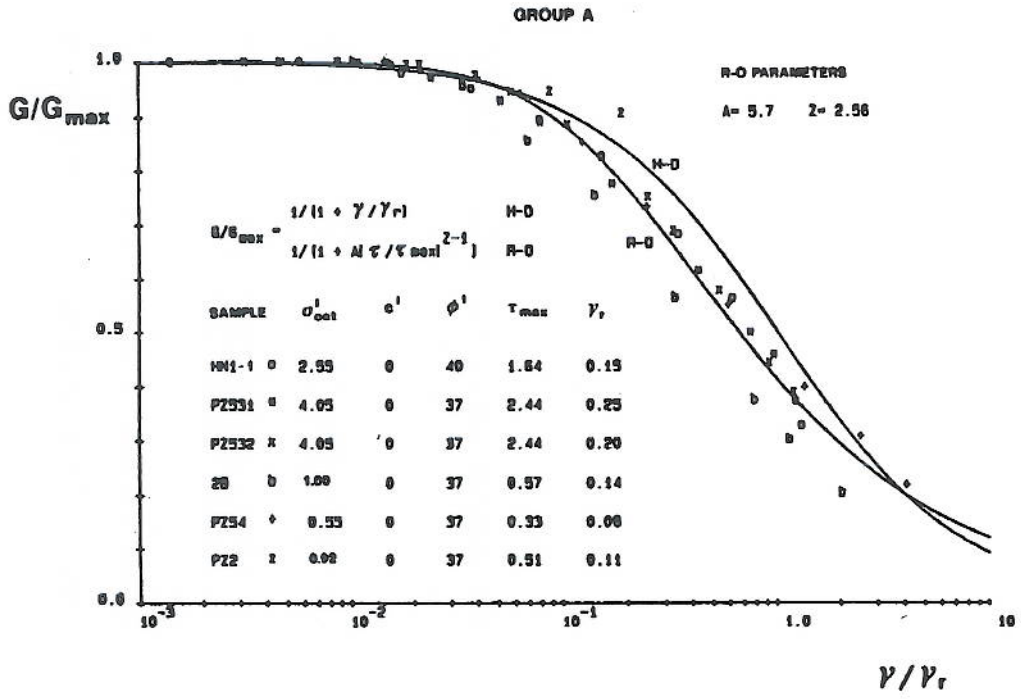

Fig.18

Dependence of normalized shear modulus G/G_{max} on normalized cyclic shear strain amplitude γ/γ_r, from resonant column tests on samples of TBJ (Group A) soils. Curves are data fits by the hyperbolic (H-D) and Ramberg-Osgood (R-O) models given in the figure, with $\gamma_r = \tau_{max}/G_{max}$ and τ_{max} = limit shear stress (in kg/cm^2).

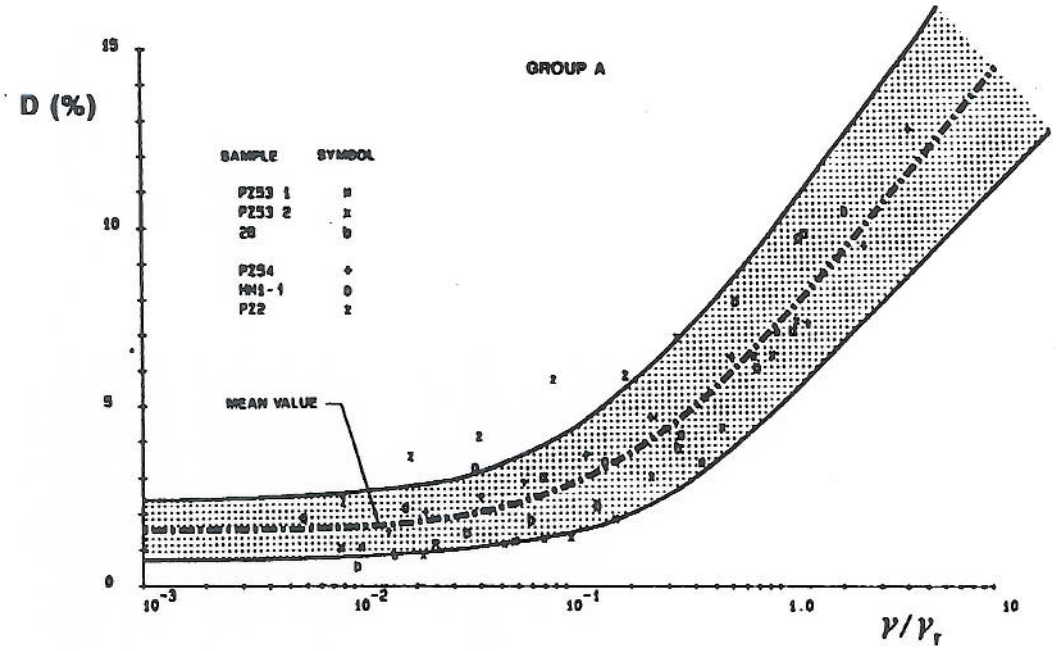

Fig.19

Dependence of internal damping coefficient D on normalized cyclic shear strain amplitude γ/γ_r, defined in Fig.18, from resonant column tests on samples of TBJ (Group A) soils. Stippled band visualizes typical data dispersion.

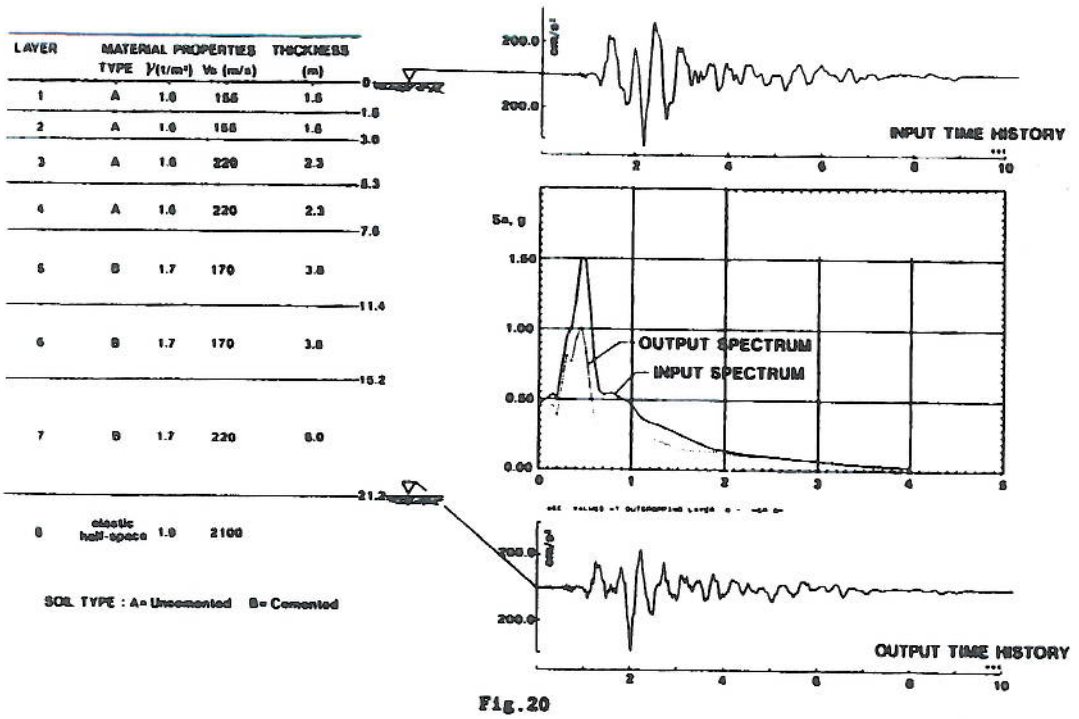

Fig.20

Soil profile and deconvolution analysis at accelerograph site HCR using the SH component of 1986 HCR (basement) recording.

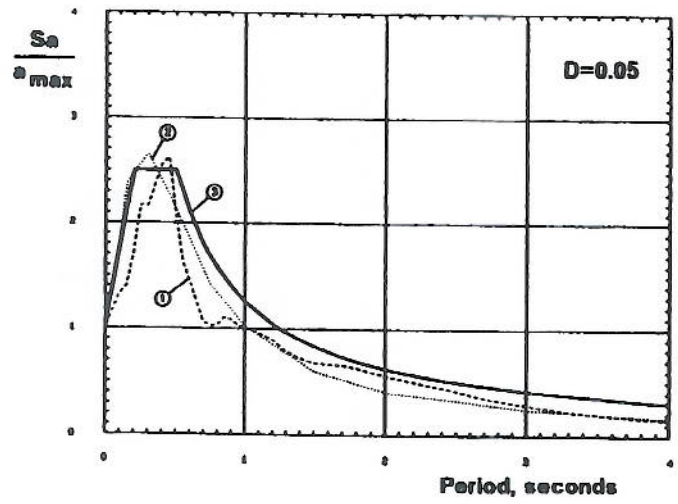

Fig.21

ERS shapes for Zone 1A. 1-average from deconvolutions at HCR, HSH, UCA sites; 2-mean shape from Joyner and Boore (1982) correlations for M=6.5, d=0, rock sites; 3-proposed envelope.

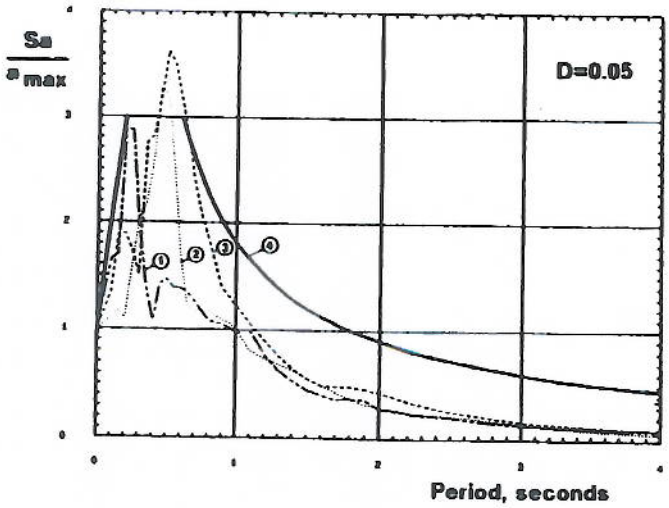

Fig.22

ERS shapes for Zone 1B.
1-HSH, comp.SH; 2-HCR, comp.SH; 3-UCA, comp.SH; 4-proposed envelope.

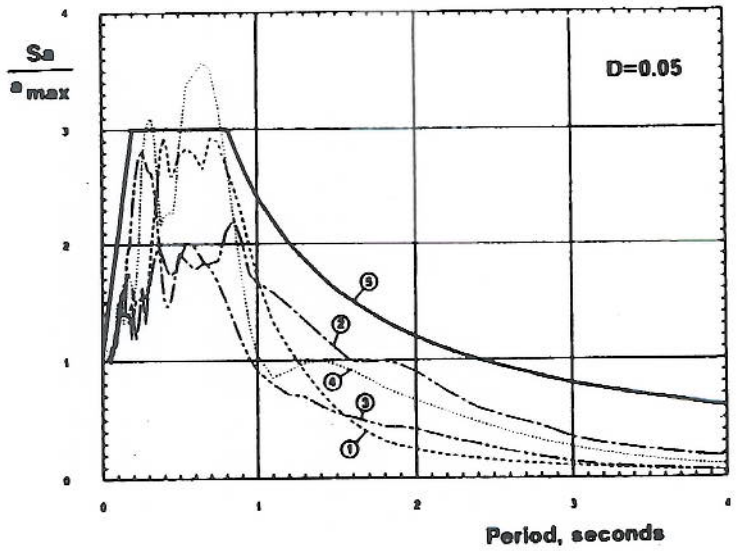

Fig.23

ERS shapes for Zone 2.
1-IGN, comp.WE; 2-IGN, comp.SN
3-CIG, comp.EW; 4-CIG, comp.SN
5-proposed envelope.

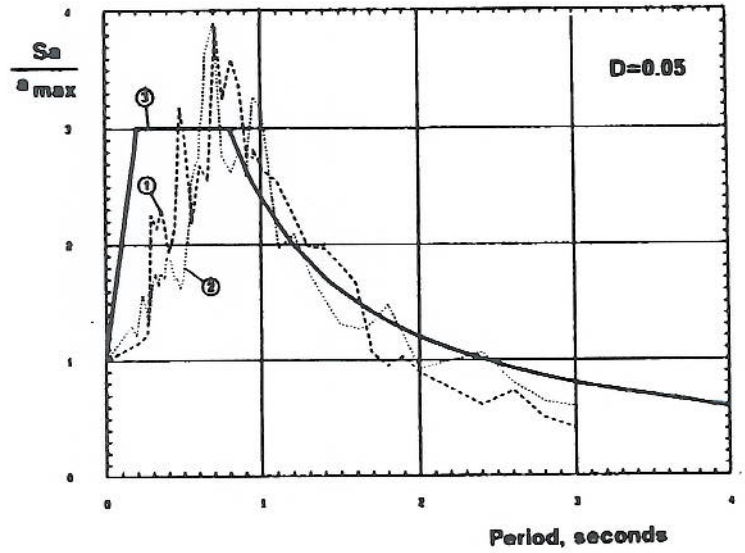

Fig.24

Verification of proposed ERS shape for Zone 2 vis-a-vis subduction zone earthquakes.
1-Observatorio, comp.EW, event of June 19, 1982;
2-Same, comp.NS;
3-Proposed envelope.

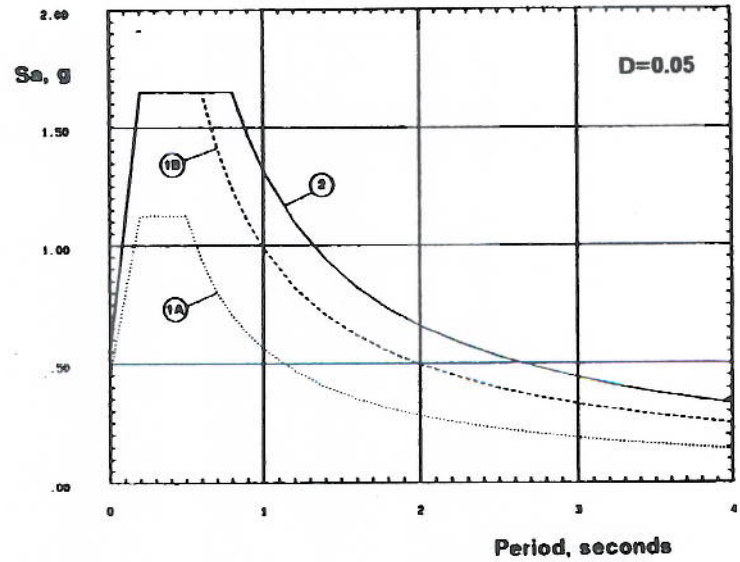

Fig.25

Comparison of the proposed ERS for the three stable subsoil zones of the study area.

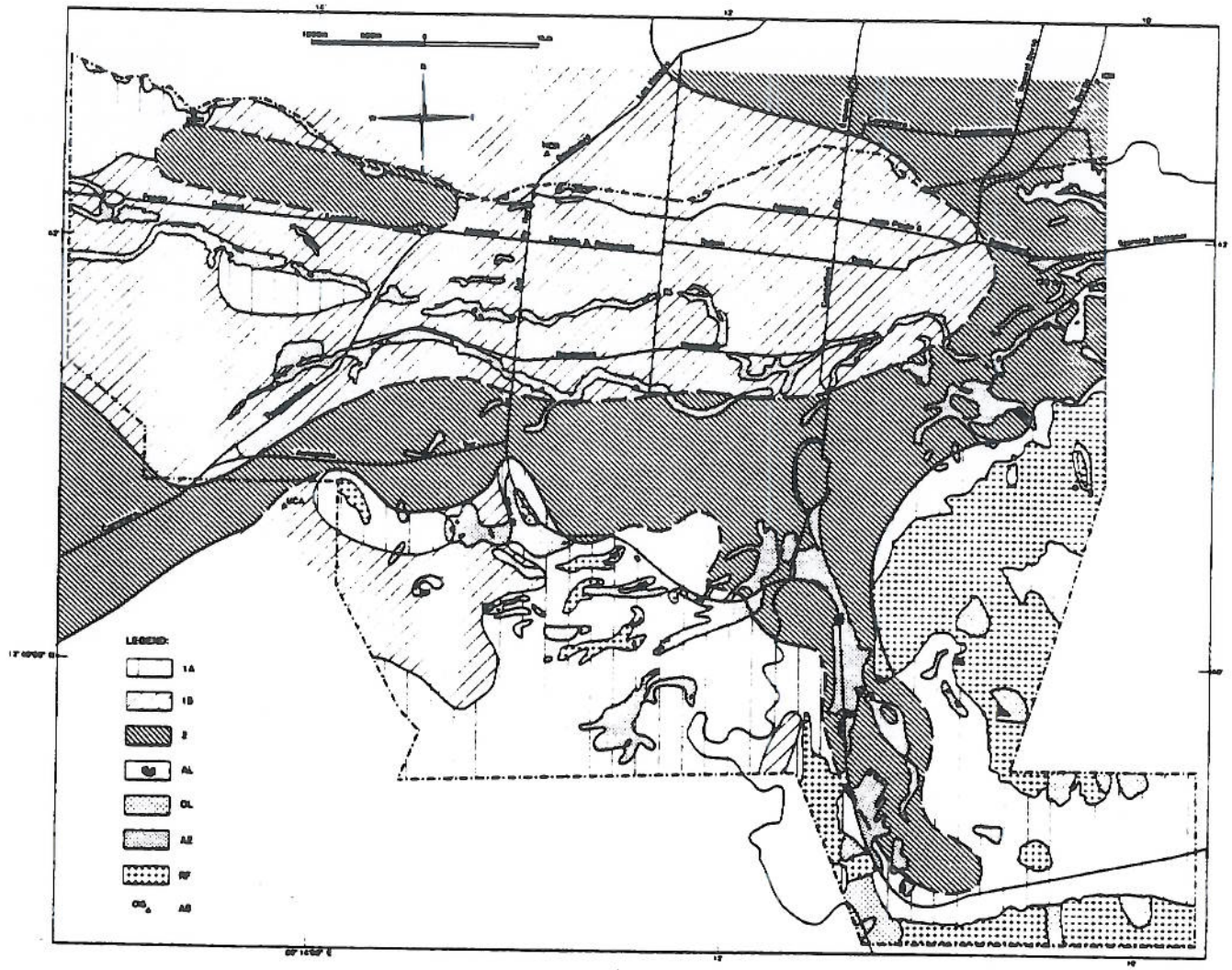

Fig.26. Proposed seismic microzoning map for the DS A3 area of AMSS. STABLE ZONES (see Figs.14-13 for subsoil characterization): 1A-Massive lava flows at 0-5 m from surface, characteristic ERS values (Fig.21) A=0.45g, T_1=0.2s, T_2=0.5s, R_o=2.5; 1B-Massive lava flows at 5-35 m from surface, ERS values (Fig.22) A=0.55g, T_1=0.3s, T_2=0.6s, R_o=3.0; 2-Sparse lava flows within 100 m from surface, ERS values (Fig.23) A=0.55g, T_1=0.2s, T_2=0.8s, R_o=3.0. UNSTABLE ZONES: AL-active landslides; OL-old landslide areas; AE-areas subject to accelerated erosion/lateral stream banks erosion; RF-areas subject to rockfalls and rockslides. AS-1988 accelerograph site.

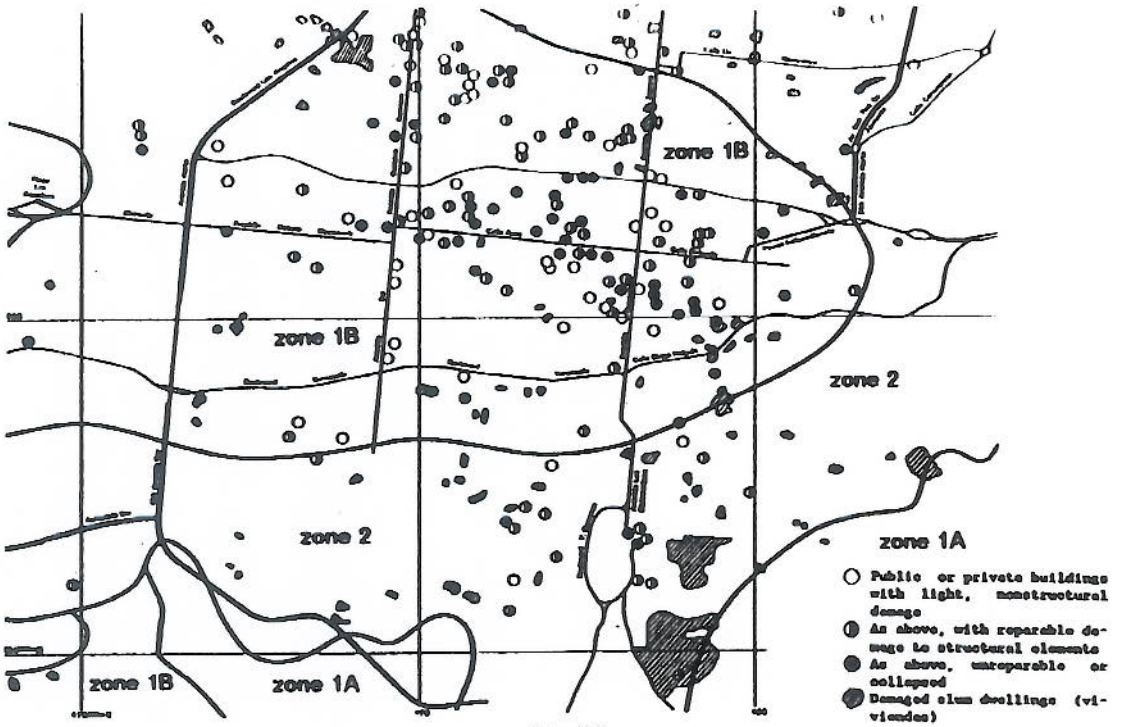

Fig.27

Damage caused by the 1986 event in central AMSS, and proposed microzones (stable soil only).

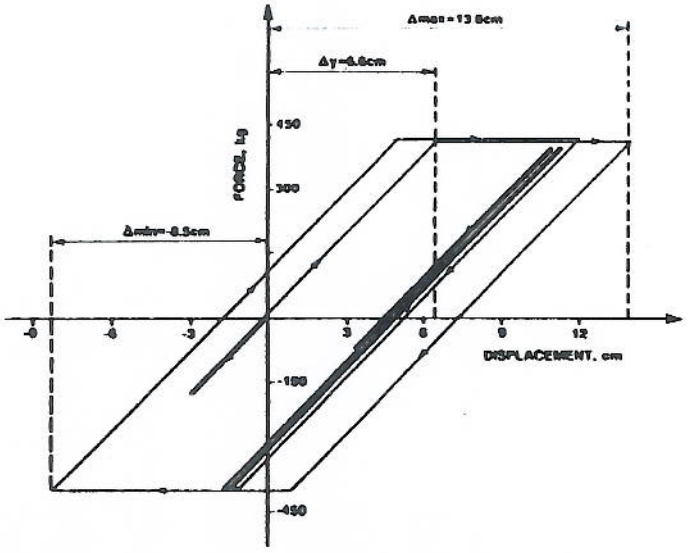

Fig.28

Force-displacement response of elastoplastic 1-DOF system (0.8s initial natural period, 0.05 damping) to 1986 IGN-EW acceleration component.

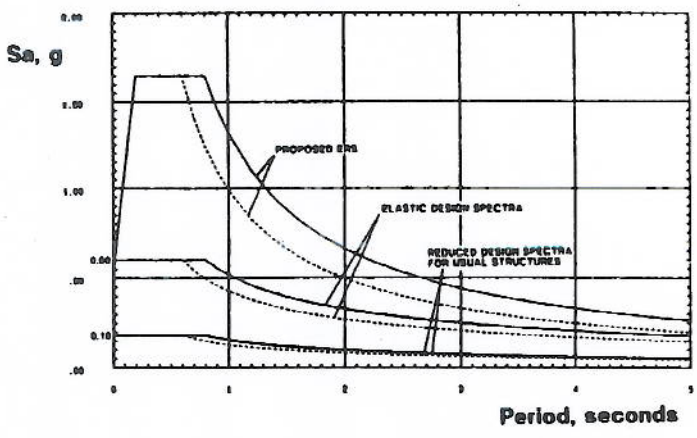

Fig.29

Proposed seismic design spectra for Zones 1B, 2, applicable to r.c. and steel structures with frames and shear walls. The elastic design spectra are reduced by a ductility factor of 10/3.